Am J Transl Res 2019;11(1):218-232
www.ajtr.org /ISSN:1943-8141/AJTR0079709

Original Article

Apogossypolone acts as a metastasis inhibitor via up-regulation of E-cadherin dependent on the GSK-3/AKT complex

Dengqiang Lin[1*], Xiaojing Wang[1*], Xiaoxia Li[2*], Li Meng[1*], Feifei Xu[1], Yunze Xu[3], Xin Xie[1], Hongchao He[1], Danfeng Xu[1], Chenghe Wang[1], Yu Zhu[1]

[1]Department of Urology, Ruijin Hospital Affiliated to Medical School of Shanghai Jiaotong University, Number 197, Ruijin'er Road, Huangpu District, Shanghai 200001, China; [2]Department of Radiology, Shanghai Ninth People's Hospital Affiliated to Medical School of Shanghai Jiaotong University, Number 639, Zhizaoju Road, Huangpu District, Shanghai 200001, China; [3]Department of Urology, Renji Hospital Affiliated to Medical School of Shanghai Jiaotong University, Number 1630, Dongfang Road, Pudong District, Shanghai 200120, China. [*]Equal contributors.

Received April 22, 2018; Accepted November 12, 2018; Epub January 15, 2019; Published January 30, 2019

Abstract: Malignant pheochromocytoma is exactly diagnosed only upon the occurrence of metastatic foci. At that point, however, patients are less likely to experience many benefits from traditional chemotherapy. Therefore, a strategy worthy of consideration is inhibition or delay of metastasis with drugs. Recently, numerous studies have indicated that epithelial-to-mesenchymal transition (EMT) is involved in malignant pheochromocytoma, where there is over-expression of metastatic promoting genes and low expression of metastatic suppressor genes. In previous research, we confirmed that apogossypolone (ApoG2) could effectively inhibit tumor movement capabilities, but potential mechanisms for the inhibition were unknown. Here, we initially corroborated that ApoG2 could induce GSK-3/AKT complex formation to down-regulate phosphorylation of the PI3K/AKT pathway. Subsequently, ApoG2 inhibited cell mobilities via promotion of E-cadherin and β-catenin translocation from cytoplasm to membrane dependent on down-regulate of the PI3K/AKT pathway. Unexpectedly, ApoG2 seemed to promote tumor progression, instead of suppression when there were circulating tumor cells *in vivo*. Our results indicated that ApoG2 might be an effective target agent early in the disease rather than at the advanced stage where there are a majority of circulating tumor cells. Those cells rely on the mesenchymal-epithelial transition (MET) process to anchor to distant new sites. Hence, the so-called anti-tumor drugs with inhibition of migration and invasion should be carefully distinguished as to whether they are involved in EMT and MET processes or not. Most importantly, we identified that GSK-3 is not only a downstream effector but also an upstream regulator of the PI3K/AKT pathway.

Keywords: Pheochromocytoma, apogossypolone, epithelial-mesenchymal transition, mesenchymal-epithelial transition, E-cadherin

Introduction

Pheochromocytoma (PHEO) is a rare but life-threatening neuroendocrine tumor associated with catecholamine production. It usually arises from chromaffin cells of the adrenal medulla. The estimated yearly incidence of PHEOs ranges from 2 to 8 cases per million [1, 2]. Among patients with PHEO, the prevalence of malignancy is between 3% and 36% [3]. Early radical surgical resection is seen as the only means of cure until recently. Compared with the 84-96% 5-year survival rate for benign PHEO, the 5-year survival rate for the malignant form is poor at less than 50% [4-6], and the recurrence rate post operation is 65.4% within 5 years [7]. Worse still, owing to limited early identification of malignant PHEO, the majority of patients are diagnosed with malignant PHEO solely on the presence of metastatic lesions [8]. Hence, they regrettably miss the optimal treatment opportunity. Tumor metastasis is the main obstacle in the treatment of PHEO. Therefore, novel effective agents to inhibit or delay metastasis are urgently required for malignant PHEO.

Cancer metastatic dissemination, accounting for more than 90% of cancer-specific deaths, is closely related to tumor cell motility [9, 10]. Epithelial-to-mesenchymal transition (EMT) is a normal process during embryonic development but is abnormally reactivated during tumor progression and thereby tumor acquires motility properties [11, 12]. During EMT, the loss of epithelial markers (E-cadherin and β-catenin) on the membrane and the acquisition of mesenchymal markers (vimentin, Twist and Snail) contributes to the loss of cell-cell and cell-matrix adhesion properties leading to tumor migration and invasion [13]. Recently, numerous studies have indicated that EMT is involved in malignant PHEO. Overexpression of Twist and Snail have been frequently observed in the malignancy [14]. In addition, Ohta *et al*. [15] implied that 6 of 11 metastasis suppressor genes (E-Cad, nm23-H1, TIMP-4, BRMS-1, TXNIP and CRSP-3) were statistically significantly down-regulated in malignant PHEO compared to benign PHEO.

Our previous study demonstrated that apogossypolone (ApoG2), an inhibitor targeting to BCL-2 family proteins, could inhibit pheochromocytoma cell line (PC12) migration and invasion [16]. However, the underlying mechanism remains unclear. Our preliminary experiment suggested that decreased movement induced by ApoG2 might be due to reversing the EMT process. Therefore, we further sought to investigate the above mechanism, potentially helping to improve the prognosis of patients with PHEO.

Materials and methods

Cell line and chemical reagents

The PC12 cell was originally donated by the Institute of Neurology in Ruijin Hospital affiliated to the Medical School of Shanghai Jiaotong University, China. Apogossypolone (ApoG2) was purchased from ApexBio (Houston, USA). On the day of an experiment, ApoG2 powder was diluted to 20 mmol/L stock solution with pure dimethyl sulfoxide (DMSO; Sigma, California, USA), and subsequently diluted to the appropriate working solution concentration with culture medium. Primary antibodies (E-cadherin, vimentin, β-catenin and so on) were purchased from Cell Signaling Technology (Boston, USA), and protein extraction kits were provided by Beyotime Company (Shanghai, China). Double-stranded RNA (dsRNA) and small interfering RNA (siRNA) of E-cadherin were purchased from Ribobio (Guangzhou, China).

Cell culture

PC12 cells were cultured in 60-cm^2 dishes in an incubator under conditions of 37°C, 5% CO_2, and 90% humidity. The medium for PC12 cells comprised 5% fetal bovine serum (FBS, Thermo Fisher Scientific, Massachusetts, USA), 10% horse serum (Thermo Fisher Scientific, Massachusetts, USA), and 85% dulbecco's modified eagle medium (DMEM). PC12 cells were subcultured or the culture medium was replaced every 3 days.

Wound healing assay and Transwell assay

Approximately 4×10^6 cells were seeded into each well of a six-well plate. After incubation for 24 h, the confluent cell monolayers were scratched with a 10 μL sterile pipette tip. Non-adherent cells were then washed off with sterilized phosphate-buffered saline (PBS), and serum-free medium with corresponding treatment was added into the wells. The width of scratch was measured using an inverted microscope (Olympus, Tokyo, Japan). Three random non-overlapping areas in each well were pictured at 0, 12, 24 and 48 h post scratch.

Tumor cell migration was assayed in Transwell chambers (Corning, New York, USA) and the membrane used for the invasive assay was purchased from BD. Briefly, PC12 cells at a density of 1×10^5 per well were seeded into upper Transwell chambers with or without ApoG2 diluted in 200 μL DMEM, and 10% FBS media were added to lower Transwell chambers. After incubation for 6 h in a 37°C incubator, cells were fixed with methanol for 15 min and then stained with crystal violet for 15 min. Cells on the upper surface of the filter were then carefully wiped away with a cotton swab and the cells on the lower surface of the filter were counted using an inverted microscope.

Protein extraction and western blotting

Cells were harvested, washed twice with PBS, and then lysed in ice-cold lysis buffer containing 1% phenylmethylsulfonyl fluoride (PMSF) and 10% protease-inhibitor cocktail, for 30 min at 4°C. Cell lysates were centrifuged at 12000 r.p.m. for 30 min to remove precipitate, loading

buffer was added, and samples were stored at -20°C until use. Proteins were separated by SDS-PAGE (10 or 12% gels) and transferred to polyvinylidene fluoride (PVDF) membranes (Millipore, USA). Non-specific binding sites were blocked with 5% Bovine serum albumin (BSA) for 1 h at normal atmospheric temperature, and subsequently membranes were incubated overnight at 4°C with primary antibodies (1:1000) and β-actin (1:2000). Membranes were then washed three times with PBS-T (PBS with 1‰ Tween-20) and incubated with corresponding secondary antibodies at room temperature for 40 min. After washing three times with PBS-T, protein bands were detected using the enhanced chemiluminescence method and Image Lab software (Bio-Rad).

Immunofluorescence

Briefly, PC12 cells seeded onto glass slides were treated with or with ApoG2. After treatment for 24 h, the slides were washed with PBS, cells were fixed with 4% paraformaldehyde for 15 min, permeated with 0.3% Triton X-100 in PBS for 15 min at room temperature, and blocked for 1 h with 5% BSA in PBS. The cells were then stained with corresponding primary antibodies (1:200 dilution) overnight at 4°C. After washing three times with PBS-T, cells were stained with corresponding secondary antibodies and a 4',6-diamidino-2-phenylindole (DAPI) nuclear stain (Beyotime, Shanghai, China). The slides were viewed under an Olympus microscope.

Cell transfection

The day before transfection, cells were treated with trypsin, seeded into new six-well plates at a density of 50-60% and then cultured without antibiotics. All dsRNA/siRNA was transfected with Lipofectamine RNAiMax (Thermo Fisher Scientific, Massachusetts, USA) in Opti-MEM medium according to the manufacturer's instructions.

Co-immunoprecipitation (Co-IP)

Briefly, PC12 cells were lysed with cell lysis buffer for Western and IP (Beyotime, Shanghai, China) and centrifuged at 12000 r.p.m. for 30 min. The supernatants were then incubated with corresponding antibodies (1:100) overnight at 4°C. Protein G agarose beads prewashed with lysis buffer were used to capture antibodies at room temperature for 2 h. Cell lysates were centrifuged at 12000 r.p.m. for 30 min to segregate precipitate from lysates, and the supernatants served as negative controls. Proteins bound to the beads were heated to denature compounds before separation and analysis by SDS-PAGE and Western blotting.

Mouse metastasis model

PC12 cells with Lenti-Luciferase or Lenti-Control (5×10^5, 100 μL) were intravenously injected via the tail vein into female athymic nude mice (Shanghai Institute of Material Medical, China) at 4 weeks of age. The next day, mice were randomized to two groups: control and treatment. The treatment group received ApoG2 by intraperitoneal injection at 20 mg/kg every day; the expected duration of treatment was 30 days but actual duration was 23 days. Mice weights were monitored every day. At 30 days, the incidence and volume of metastases should have been estimated through *in vitro* imaging with the Living Image software.

Immunohistochemistry and hematoxylin and eosin (H&E) staining

After fixing in 10% neutral formalin and dehydrating in an alcohol concentration gradient, samples were embedded in paraffin, then cut into 3-μm serial sections, which were dewaxed twice in xylene, rehydrated in alcohol, and then rinsed with PBS followed by treatment with 3% H_2O_2 for 10 min to inactivate endogenous peroxidase. After antigen retrieval, the slides were incubated with 10% goat serum for 10 min under constant temperature to block non-specific reactions. Subsequently, sections were treated with polyclonal rabbit anti-human Bcl-2 and Bax antibody for 12 h at 4°C. After washing with PBS three times, the slides were incubated with secondary antibody at 37°C for 30 min. Slides were then washed again with PBS, developed in diaminobenzidine (DAB) substrate, counter-stained with hematoxylin, and dehydrated with ethanol and xylene before being mounted. For negative controls, the slides were incubated with PBS instead of primary antibodies.

The above sections were deparaffinized with xylene, hydrated through a graded ethanol series, stained with H&E, dehydrated through a graded ethanol series, cleared in xylene, and finally mounted in neutral resin. Pathological and morphological changes were observed under a light microscope (Olympus, Tokyo, Japan).

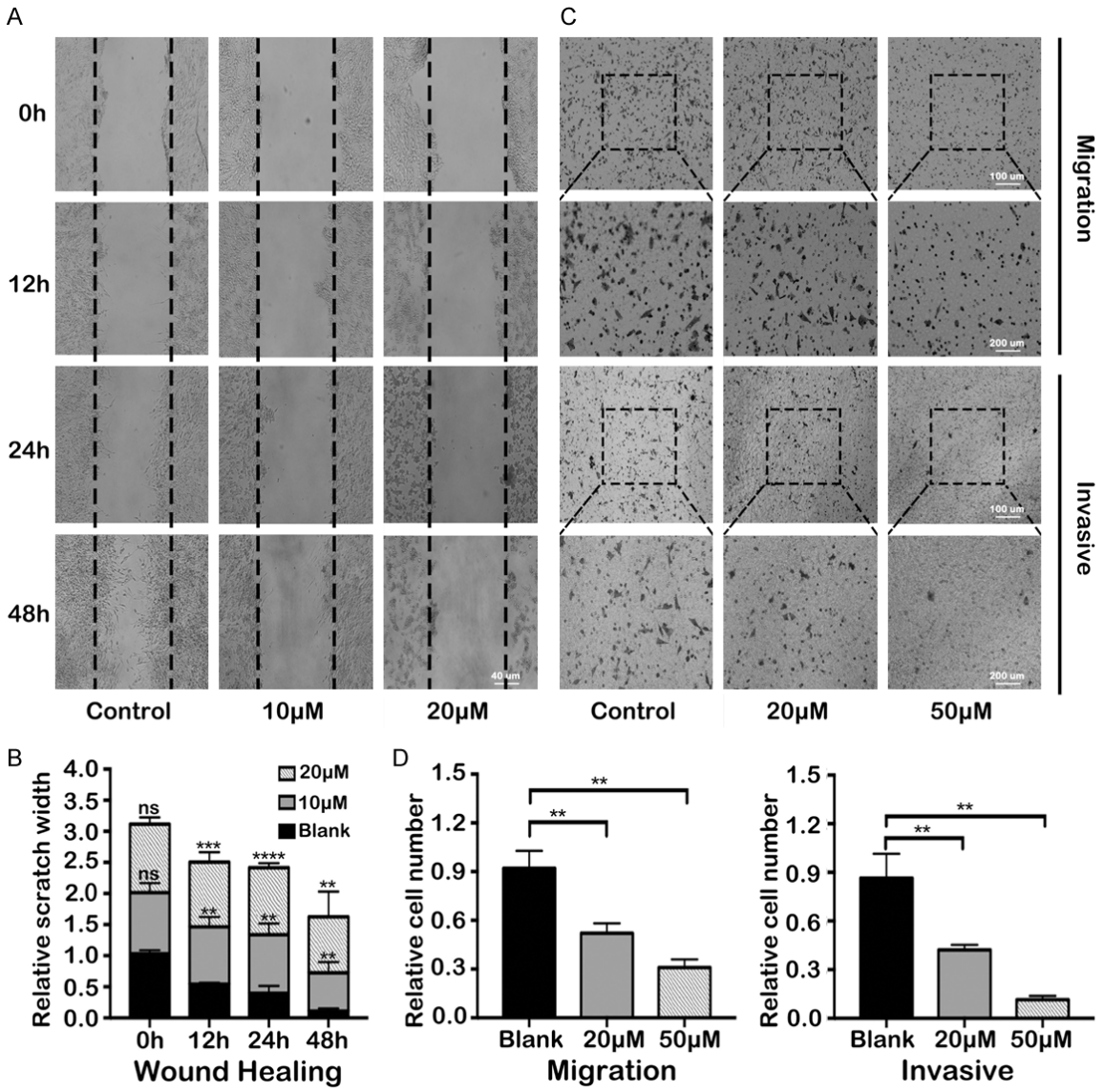

Figure 1. A and B. ApoG2 inhibits migration and invasion in PC12 cells as assessed by using a wound healing assay. Relative scratch width of three groups were 0.11 ± 0.04, 0.62 ± 0.17 and 0.90 ± 0.41 at 48 h, respectively. C and D. ApoG2 inhibits migration and invasion in PC12 cells as assessed by using a Transwell assay. Relative cell number of three groups in migration assay were 0.92 ± 0.11, 0.52 ± 0.06 and 0.31 ± 0.05, respectively. And relative cell number of three groups in invasive assay were 0.86 ± 0.15, 0.42 ± 0.03 and 0.11 ± 0.02, respectively. No statistical significance (ns), $P > 0.05$; **, $P < 0.01$; ***, $P < 0.001$; ****, $P < 0.0001$.

Statistical analysis

All data are presented as means ± standard deviation. Statistical analyses were performed with SPSS 21.0 software (IBM) and corresponding bar graph or line charts were drawn by GraphPad Prism 7 software. Differences of measurement data and enumeration data were compared respectively with Student's *t*-test, chi-square test, and analysis of variance. A Kaplan-Meier survival plot was generated to compare overall survival with the log-rank statistic. *P* values less than 0.05 were considered as statistically significant. Scratch width, maximum diameter of metastatic focus, alveolus area, and so on were quantified by Image J software.

Results

ApoG2 suppressed PC12 cell migration and invasion

In order to evaluate the effects of ApoG2 on migration and invasion, a wound-healing test was performed. After the wound widths of each

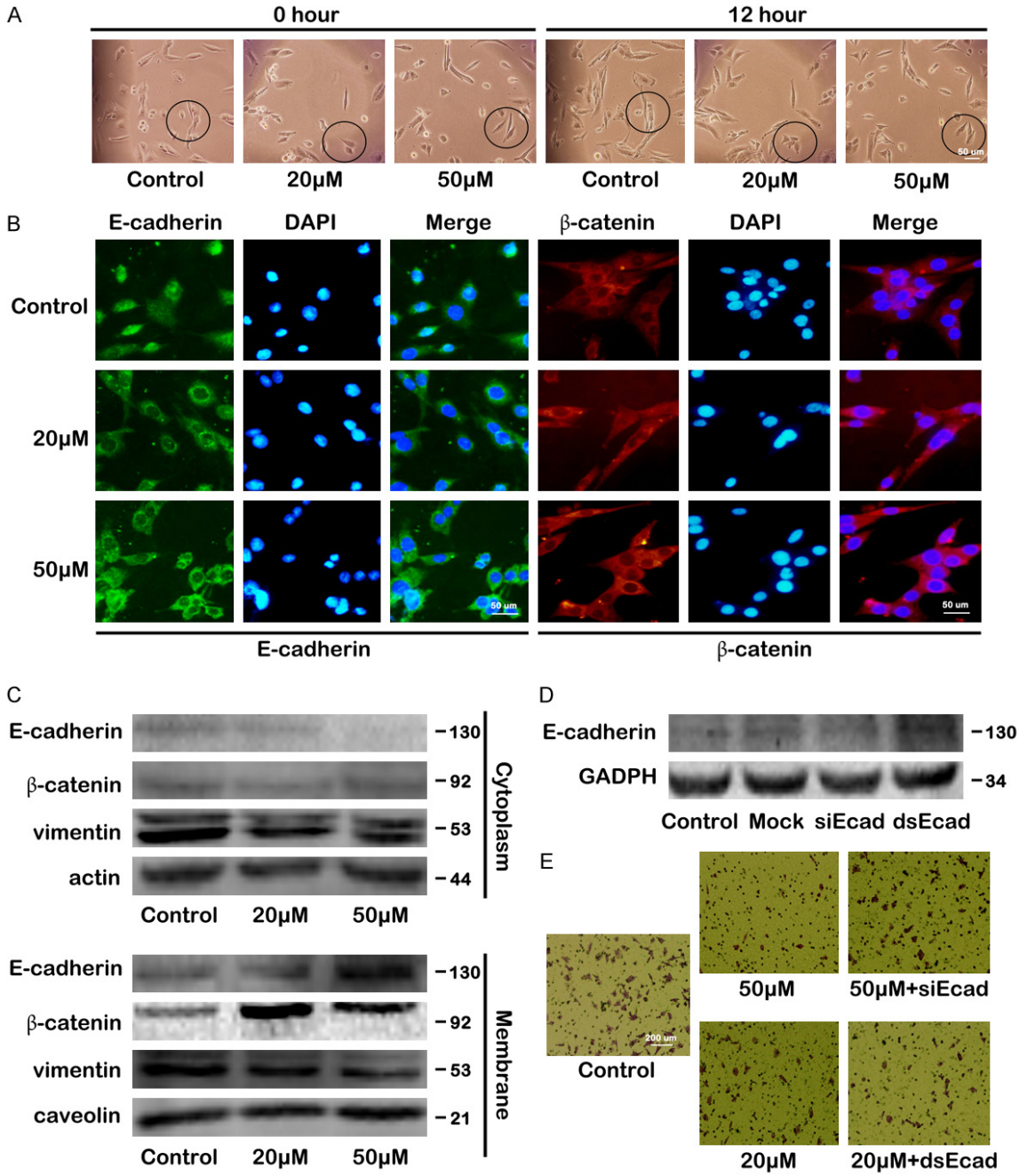

Figure 2. ApoG2 suppression of EMT is dependent on E-cadherin. A. Results of morphological characteristics of cells showed that some of the cells in the ApoG2-treated group always sustained epithelioid morphology such as a small, round or polymorphic phenotype instead of a stroma-like phenotype. B. In the ApoG2-treated group, cytoplasmic staining and peripheral staining of E-cadherin and a stronger stain of β-catenin were observed compared with the matched group assessed by immunofluorescence staining. C. E-cadherin and β-catenin gradually translocated from cytoplasm to membrane and vimentin decreased in both cytoplasm and membrane fractions as dose of ApoG2 increasing. D. E-cadherin was silenced by siRNA and over-expressed by dsRNA. E. Knockdown of E-cadherin could significantly reverse the ApoG2 effect, and conversely, over-expression of E-cadherin could significantly strengthen the ApoG2 effect.

group were normalized to the corresponding control group at 0 h, the results suggested that ApoG2 could significantly inhibit cell migration from 12 h post treatment (**Figure 1A** and **1B**). These results were further attested by Transwell assays. As illustrated in **Figure 1C** and **1D**,

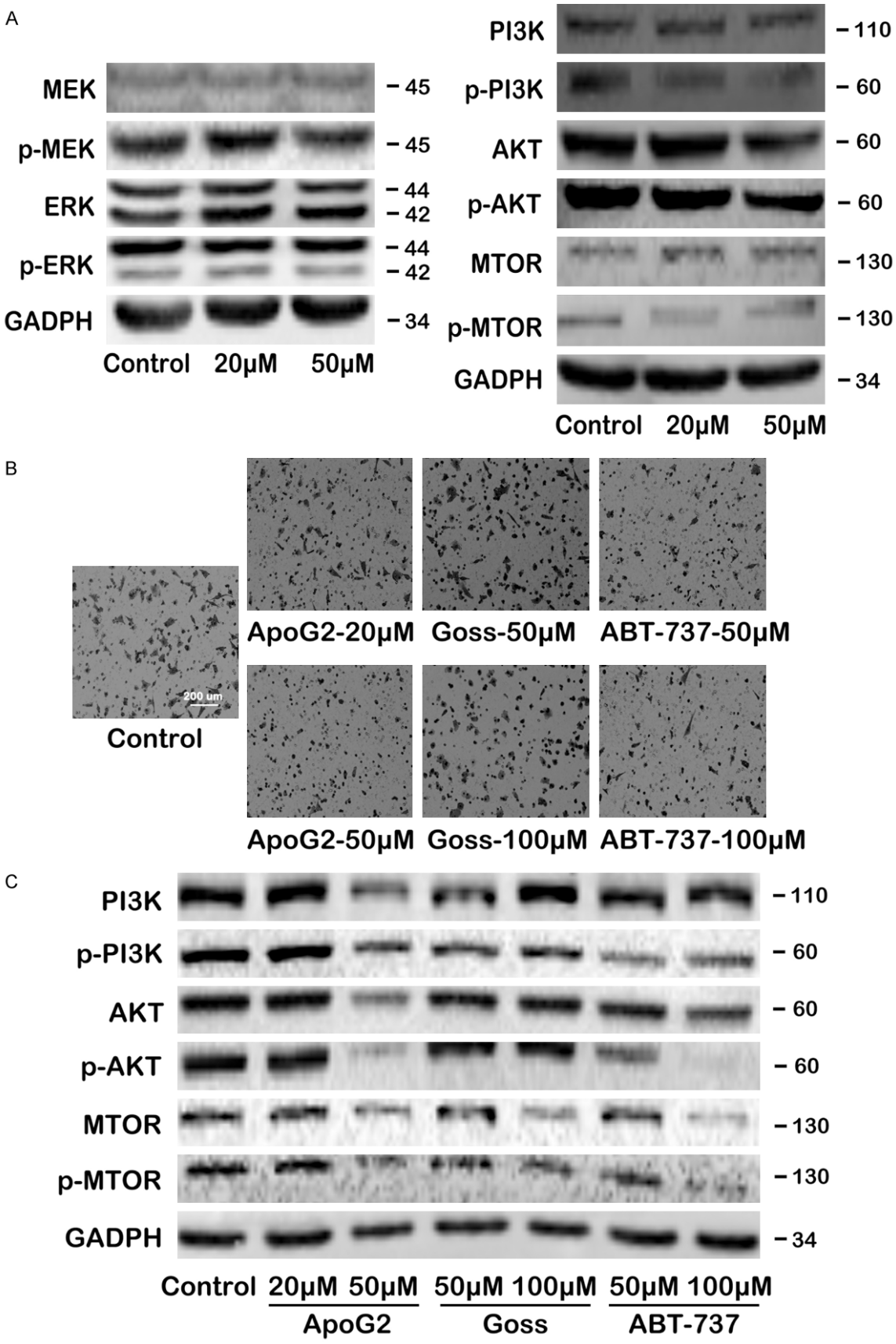
A
MEK
p-MEK
ERK
p-ERK
GADPH
45
45
44
42
44
42
34
Control
20μM
50μM
PI3K
p-PI3K
AKT
p-AKT
MTOR
p-MTOR
GADPH
110
60
60
60
130
130
34
Control
20μM
50μM
B
200 um
Control
ApoG2-20μM
Goss-50μM
ABT-737-50μM
ApoG2-50μM
Goss-100μM
ABT-737-100μM
C
PI3K
p-PI3K
AKT
p-AKT
MTOR
p-MTOR
GADPH
110
60
60
60
130
130
34
Control
20μM
50μM
50μM
100μM
50μM
100μM
ApoG2
Goss
ABT-737

Figure 3. ApoG2 suppresses activation of the PI3K/AKT signaling pathway. A. ApoG2 inhibits phosphorylation of the PI3K/AKT pathway rather than the MEK/ERK pathway. B. After comparison of anti-EMT effect with three analogs targeted to the BCL-2 family, we found that ApoG2 and ABT-737 could effectively inhibit cell mobilities, but gossypol could not. C. ApoG2 and ABT-737 could inhibit phosphorylation of PI3K/AKT pathway, but Goss could not.

ApoG2 could remarkably repress cell migration and invasion capabilities.

ApoG2 suppressed EMT through up-regulation of E-cadherin in the membranes

Compared to matched groups, we observed that some of cells in ApoG2-treated groups always sustained epithelioid morphology such as a small, round or polymorphic phenotype instead of a stroma-like phenotype (**Figure 2A**). At that point, immunofluorescence analysis was carried out to further examine the distribution of epithelial hallmark E-cadherin and mesenchymal hallmark vimentin, as well as EMT-related molecular β-catenin. In the ApoG2-treated group, cytoplasmic staining and peripheral staining of E-cadherin were observed compared with diffuse staining in the matched group (**Figure 2B**). Also, β-catenin showed a stronger stain in the treated group (**Figure 2B**). Unfortunately, vimentin stain in both groups did not show any obvious differences (Supplementary Figure 1A). The results of subcellular localization experiments further strengthened the above findings. E-cadherin and β-catenin gradually translocated from cytoplasm to membrane and vimentin decreased in both cytoplasm and membrane fractions (**Figure 2C**).

ApoG2 suppression of EMT was dependent on E-cadherin

The above results strongly suggested that ApoG2 suppresses EMT in a process possibly dependent on up-regulation of E-cadherin. Subsequently, we asked whether knockdown of E-cadherin has a reverse effect and whether over-expression of E-cadherin has an additive effect. As expected, knockdown of E-cadherin by siRNA could significantly reverse the ApoG2 effect, and conversely, over-expression of E-cadherin through RNA activation technology [17] could significantly strengthen the ApoG2 effect (**Figure 2D** and **2E** and Supplementary Figure 1B).

ApoG2 suppression of EMT was dependent on the PI3K/AKT signaling pathway

To assess which pathway was involved in the EMT suppression effect of ApoG2, two prominent signaling pathways, PI3K/AKT and MEK/ERK [18-20], were tentatively evaluated by Western blotting. As shown in **Figure 3A**, ApoG2 could significantly inhibit phosphorylation of PI3K/AKT but not MEK/ERK. However, further investigation was needed as to whether the PI3K/AKT pathway really played an indispensable role in the ApoG2 anti-EMT effect. After comparison of anti-EMT effect with three analogs targeted to the BCL-2 family, we found that ApoG2 and ABT-737 shared the same function, but gossypol did not (**Figure 3B**). Interestingly, the PI3K/AKT pathway was inhibited both after treatment with ApoG2 or after ABT-737 treatment, but not after treatment with gossypol (**Figure 3C**).

The above findings indirectly indicated that PI3K/AKT played a role in the anti-EMT effect, but they did not support the view that this was a crucial role. Subsequently, the PI3K/AKT pathway was activated with different concentrations of insulin [21]. **Figure 4A** showed the PI3K/AKT pathway was activated by insulin, and 0.5 mg/mL insulin was selected for use in further experiments. After addition of insulin, the ApoG2 anti-EMT effect was reversed in the wound-healing assay. Although there was no statistical difference in the 20 μM ApoG2 group with or without insulin (**Figure 4B** and **4C**), the results that showed insulin could reverse the ApoG2 anti-EMT effect were further confirmed via Transwell assay (**Figure 4D** and **4E**).

ApoG2 promoted E-cadherin and β-catenin translocation from cytoplasm into the membrane dependent on the GSK-3/AKT complex

To establish the relationship between the PI3K/AKT pathway and E-cadherin or β-catenin, a Co-IP assay was performed. As depicted in **Figure 5A**, ApoG2 could increase the level of

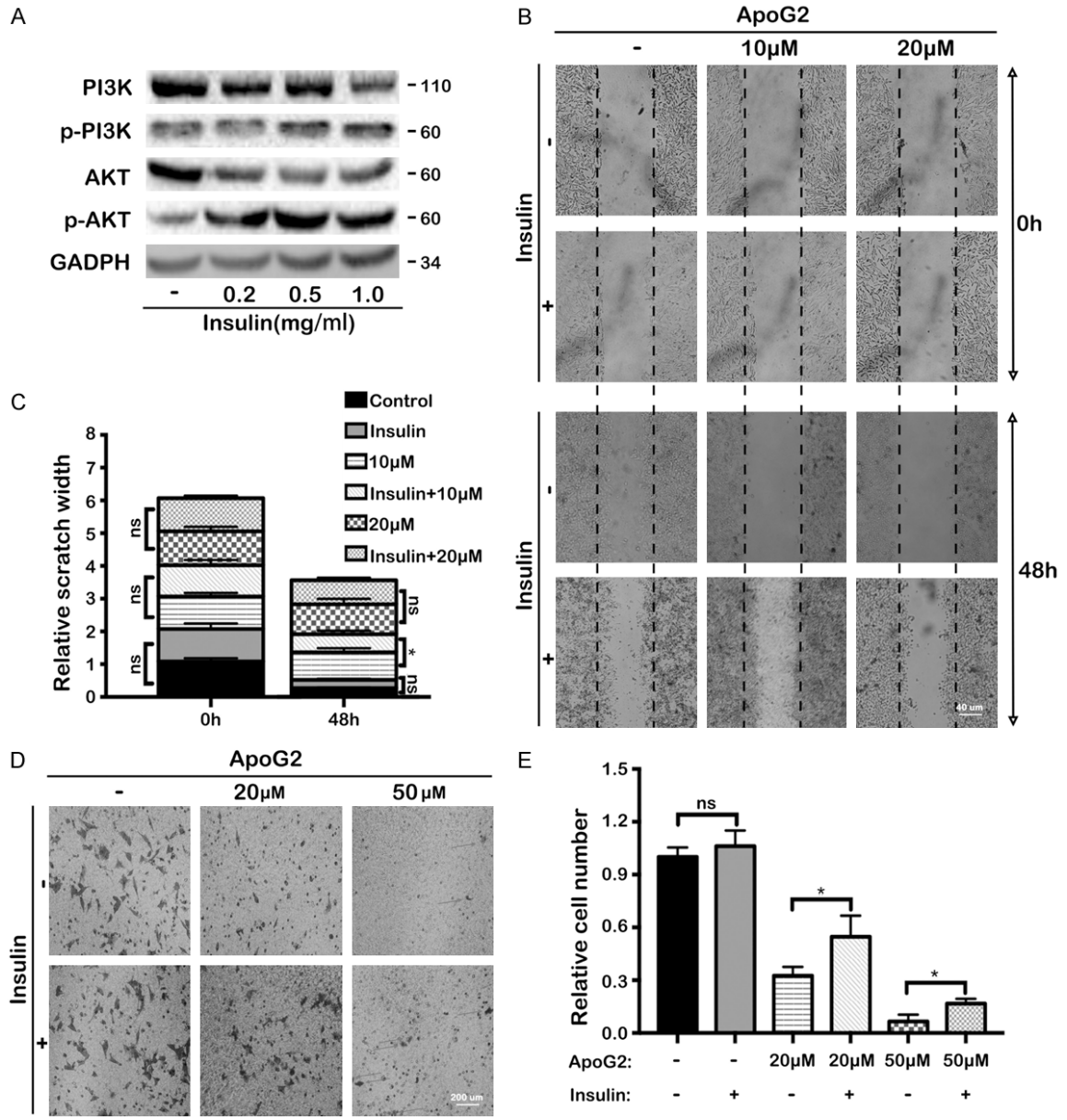

Figure 4. ApoG2 suppression of EMT is dependent on the PI3K/AKT signaling pathway. A. Insulin could activate the PI3K/AKT pathway. B, C. After addition of insulin, the ApoG2 anti-EMT effect was reversed in the wound-healing assay. After treatment of 20 μM ApoG2 for 48 h, relative scratch width in the group without insulin was 1.01 ± 0.08 compared to 0.73 ± 0.08 in the group with insulin. D and E. After addition of insulin, the ApoG2 anti-EMT effect was reversed in the Transwell assay. After treatment of 50 μM ApoG2, relative cell number in the group without insulin was 0.07 ± 0.04 compared to 0.17 ± 0.03 in the group with insulin. No statistical significance (ns), $P > 0.05$; *, $P < 0.05$.

GSK-3/AKT complex. However, ApoG2 unusually decreased the expression level of non-phosphorylated GSK-3. According to another researches, GSK-3 targeted β-catenin for degradation via ubiquitination and subsequently prevents its nuclear translocation (mesenchymal marker). To exclude the above possibility, subcellular localization assay was utilized. **Figure 5B** showed that reduced GSK-3 induced by ApoG2 could guide β-catenin into the membrane rather than the nucleus. In addition, EMT-inducing transcription factors Twist but not Zeb-1 decreased after treatment with ApoG2. Based on the above results, we sus-

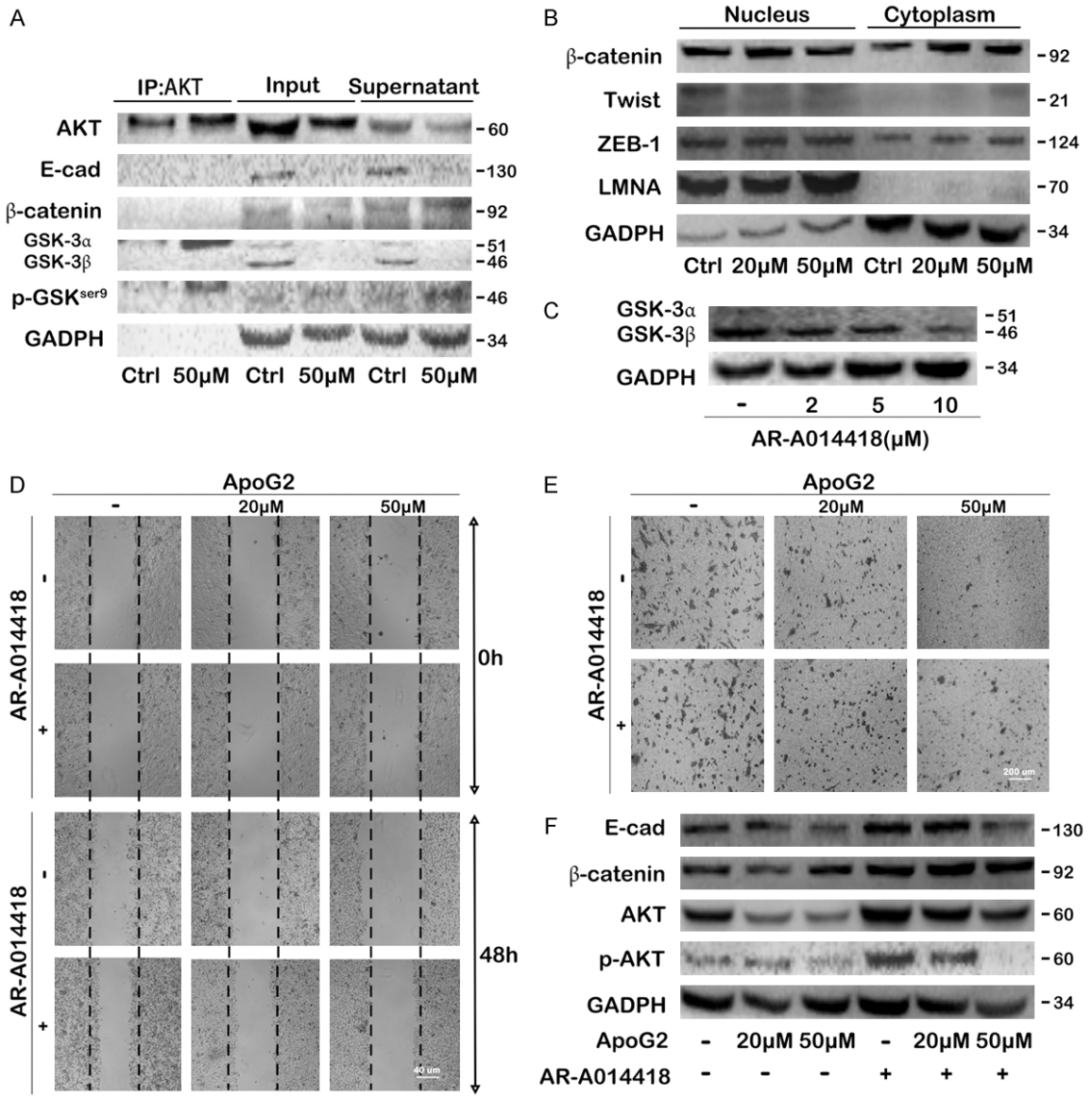

Figure 5. ApoG2-induced translocation of E-cadherin and β-catenin into membrane is dependent on the GSK-3/AKT complex. A. Co-IP showing that ApoG2 could promote GSK-3/AKT complex formation. B. Decreased GSK-3 induced by ApoG2 could not increase β-catenin level in the nucleus and ApoG2 could down-regulate Twist expression. C. The GSK-3 Inhibitor, AR-A014418, could inhibit GSK-3α/β expression. D. Results of wound-healing showed that AR-A014418 could reverse the effect of ApoG2. After treatment of 20 μM ApoG2 for 48 h, relative scratch width in the group without AR-A014418 was 1.24 ± 0.07 compared to 0.92 ± 0.06 in the group with AR-A014418. E. Results of transwell assays showed that AR-A014418 could reverse the effect of ApoG2. After treatment of 50 μM ApoG2, relative cell number in the group without AR-A014418 was 0.08 ± 0.03 compared to 0.19 ± 0.03 in the group with AR-A014418. F. AR-A014418 could increase expression of PI3K/AKT, as well as expression level of E-cadherin and β-catenin in the cytoplasm to reverse the effect of ApoG2.

pected that increased GSK-3/AKT complex induced by ApoG2 could inhibit PI3K/AKT to work in EMT.

Therefore, a spectrum inhibitor of GSK-3, AR-A014418, was used to block GSK-3/AKT complex formation. From an experiment looking at different concentrations of this inhibitor (**Figure 5C**), 10 μM AR-A014418 was selected for further experiments. As shown in **Figure 5D** and **5E**, AR-A014418 could significantly relieve the effect of ApoG2 (Supplementary Figure 1C

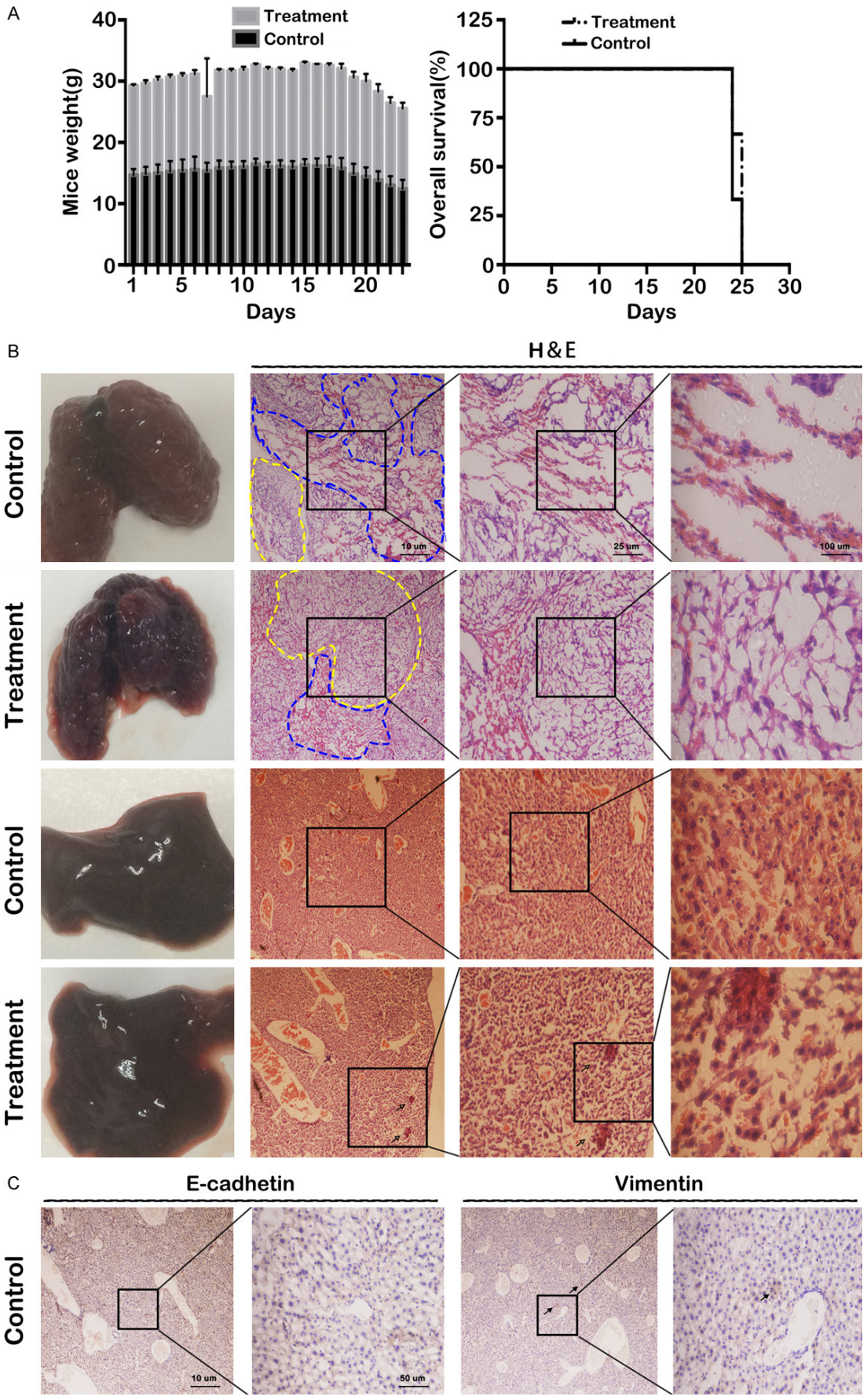
A
Treatment
Control
Mice weight(g)
Days
Overall survival(%)
Treatment
Control
Days
B
H&E
Control
Treatment
Control
Treatment
10 um
25 um
100 um
C
E-cadhetin
Vimentin
Control
10 um
50 um

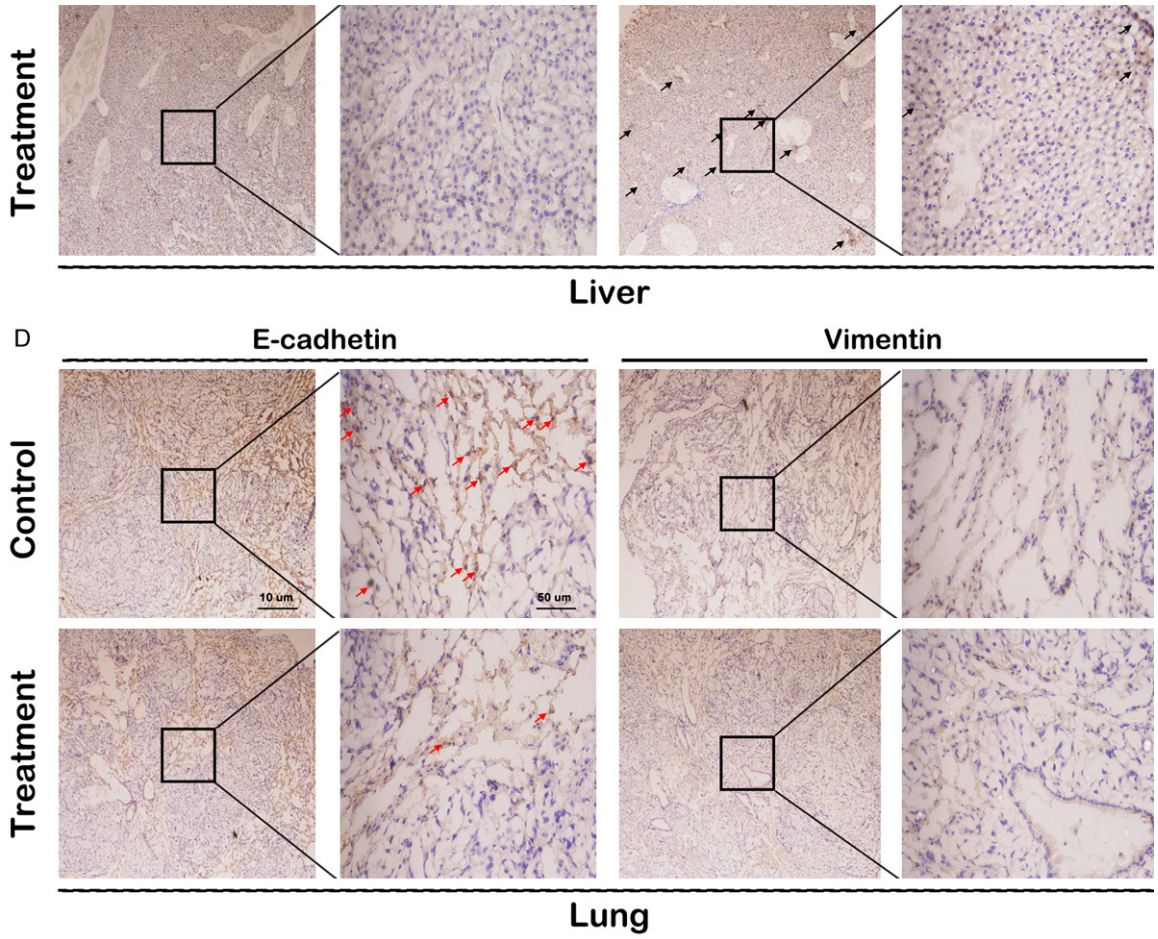

Figure 6. ApoG2 promotes rather than prevents formation of metastases in lung or liver of mice. A. The median overall survival times in ApoG2-treated mice and control mice were insignificant via Kaplan-Meier survival analysis, as were weights of mice between the two groups. B. The alveolar morphology remained clearer and metastatic foci were smaller in the control group as detected by H&E staining. Blue box, normal lung tissue; yellow box, metastatic foci. C. Immunohistochemical analysis of E-cadherin and vimentin protein expression in livers. Black arrows indicate suspicious lesions. D. Immunohistochemical analysis of E-cadherin and vimentin protein expression in lungs. Red arrows indicate dark-stained nuclei.

and 1D). Most importantly, the expression levels of phosphorylated and non-phosphorylated AKT were well rescued, and both E-cadherin and β-catenin in the cytoplasm were significantly increased (**Figure 5F**). Collectively, these results demonstrated that ApoG2 suppression of EMT was dependent on the GSK-3/AKT complex.

ApoG2 promoted rather than prevented formation of metastases in lung or liver in an in vivo experiment

Unfortunately, ApoG2 could not prevent formation of metastases in lungs or liver, and all mice died before the experimental endpoint. The median overall survival times in ApoG2-treated mice and control mice were insignificant via Kaplan-Meier survival analysis, as were weights of mice between the two groups (**Figure 6A**). Histopathological analyses revealed that lungs full of multiple nodules in both groups were insignificantly different to the naked eye, while the alveolar morphology (**Figure 6B**, blue dashed area) remained clearer and metastatic foci (**Figure 6B**, yellow dashed area) were smaller in the control group as detected by H&E staining under a microscope (**Figure 6B** and Supplementary Figure 1E and 1F). Although gross liver specimens were not covered with visible tumor nodules in both groups, liver tissues in the ApoG2 treatment group did show distribution of some suspicious micro-nodules (**Figure 6B**, black arrows). Results of anti-vimentin staining in liver tissues further supported the above viewpoint (**Figure**

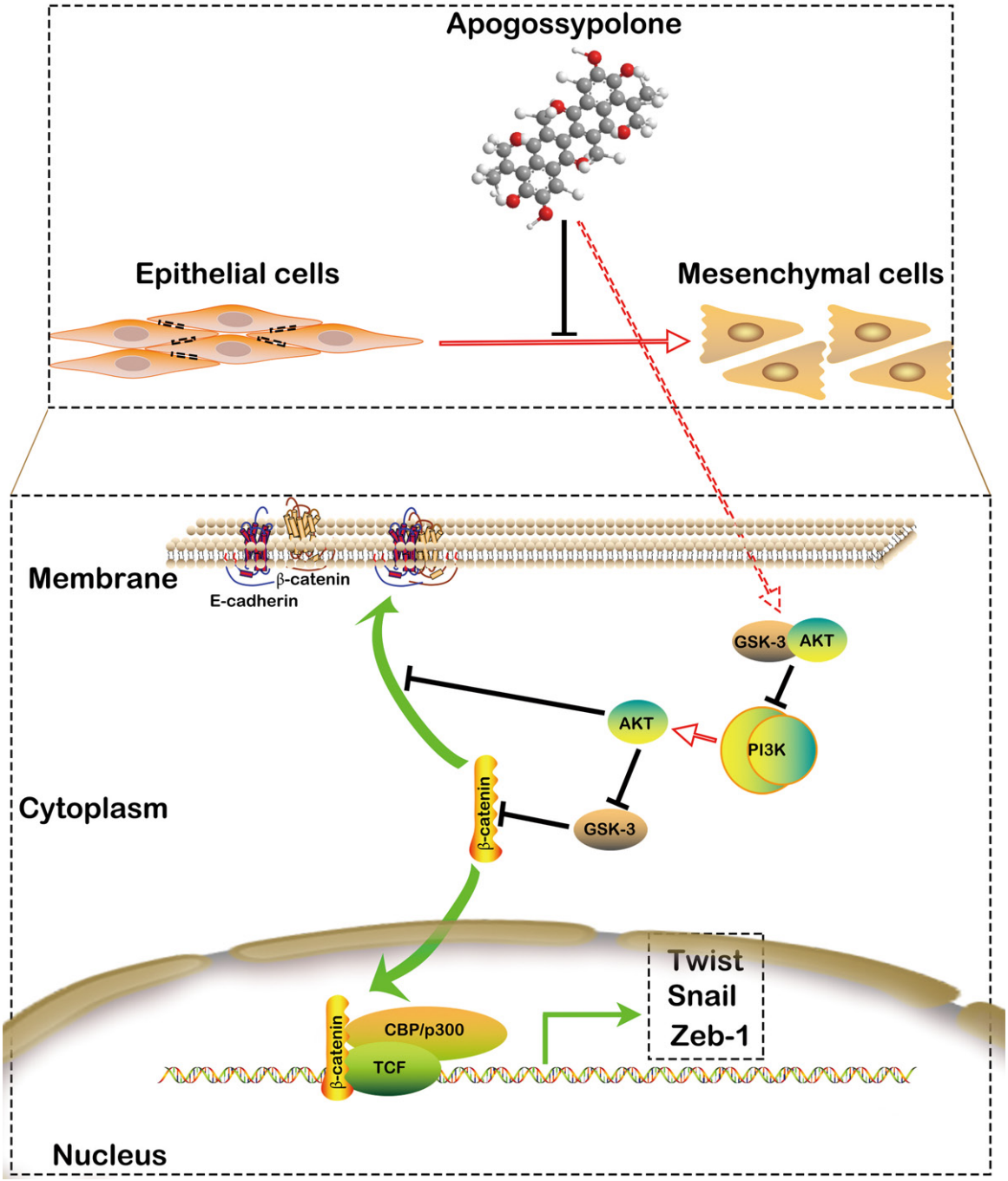

Figure 7. ApoG2 could suppress EMT through promoting translocation of E-cadherin and β-catenin from the cytoplasm to the membrane, which is dependent on GSK-3/AKT formation.

6C, black arrows). Similar to what we had observed in immunofluorescence experiments, dark-stained nucleus in the matched group were caused by E-cadherin diffuse distribution (**Figure 6D**, red arrows), in comparison with the light-stained nucleus caused by E-cadherin peripheral distribution in the ApoG2 treatment group (**Figure 6D**, red arrows), suggesting that ApoG2 had exerted efficacy *in vivo*.

Discussion

Although major efforts have been undertaken to improve the prognosis of patients with malig-

nant PHEO, those with metastasis benefit little from conventional chemotherapy. In addition, because of lack of methods to accurately distinguish the malignancy, the situation is more serious. Tumor metastasis is a prominent process determining the lethality of a malignancy and is also a major obstacle in the treatment of PHEO.

Medication, inhibition or delay of cancer metastatic progression with effective and non-toxic agents, is essential in the management of various cancers. Our previous study showed that ApoG2, targeting to BCL-2 family proteins, could induce cell apoptosis *in vitro* and *in vivo*, as well as inhibit cell invasion and cell migration [16]. However, there was no research focusing on the precise molecular mechanism of decreased cellular movement after ApoG2 treatment.

EMT has frequently been considered crucial for cancer metastasis. Generally, the E-cadherin/β-catenin complex on the cell membrane plays an important role in cell adhesion [22, 23]. Activity of β-catenin in the cytoplasm is negatively regulated by GSK-3β [23]. Once the Wnt signaling pathway is activated, β-catenin detaches from the E-cadherin/β-catenin complex in the membrane and the GSK-3/β-catenin complex in the cytoplasm, and then translocates into the nucleus where it promotes transcription of genes, such as Zeb, Twist, Slug, Snail, and so on. These factors could directly/indirectly bind to the E-box sequence in the E-cadherin promoter region to inhibit transcription, contributing to the EMT process [24, 25].

In this study, we initially corroborated that ApoG2 could inhibit tumor cell invasion and migration via a converse EMT process (**Figure 7**). Initially, ApoG2 could induce GSK-3 to detach from the GSK-3/β-catenin complex and subsequently GSK-3 binds to AKT, forming the GSK-3/AKT complex. This complex then inhibited phosphorylation of the PI3K/AKT pathway which was required for the EMT process and cell migration, as well as for participating in nuclear import of β-catenin [25, 26]. Although GSK-3 was segregated from the GSK-3/β-catenin complex, β-catenin accompanied by E-cadherin translocated from the cytoplasm into the membrane rather than the nucleus, finally leading to suppression of EMT. While precise mechanisms how the loss of GSK-3 caused reduced activation of AKT was unclear in previous studies [27, 28], our results suggested that the GSK-3/AKT complex formation caused loss of GSK-3 and then might be an upstream negative regulator of the PI3K/AKT pathway. Unfortunately, we did not elucidate the mechanism how ApoG2 induced GSK-3 to detach from the GSK-3/β-catenin complex. Furthermore, it remained unclear whether reduced expression of transcription factor Twist by ApoG2 could affect the expression level of E-cadherin.

Regarding our *in vivo* experiment, ApoG2 affected E-cadherin distribution but did not delay, and even promoted, metastatic formation. Even though this result exceeded our expectation, it was quite reasonable. Metastasis was an intricate multi-step process. Firstly, tumor cells from the primary origin degraded the surrounding matrix and invaded the bloodstream, through which they spreaded to distant sites. Subsequently, tumor cells escaped from the bloodstream into a new environment and then gave rise to a metastatic tumor [29, 30]. On the other hand, many researches had proved that the invasive property of tumor cells were actually increased via overexpression of EMT-related factors (Twist or Snail) [31-33]. However, those cells in metastatic lesions were not mesenchymal characteristics [34]. That is to say, both EMT, which increases invasive potential, and mesenchymal-epithelial transition (MET), which increases proliferation and colonization abilities to anchor to distant tissues and organs, participated in the tumor metastatic process [35-37]. In our model, PC12 cells had been artificially injected into the bloodstream. At that time, the process of MET but not EMT was crucial to form metastatic loci. Thus, it was an inevitable tendency that enhanced MET by ApoG2 promoted the establishment of metastases. Similarly, several studies supported our above analysis in different tumor types, such as those of prostate, breast, and bladder cancers [38-41].

Collectively, we reach the following conclusions when combining data from this study with our previous study. Firstly, EMT is an early step in the development of tumor metastasis, and it remains unknown whether decreased EMT by ApoG2 could delay primary tumor metastatic progression. This thought should be further confirmed by other and better models of highly aggressive tumor cells instead of PC12 cells. However, according to our previous results,

ApoG2 could effectively inhibit growth of primary tumors, at least early in the disease. Secondly, once metastasis has happened, as in our mice model in this study, the effect of ApoG2 should be carefully considered to avoid an undesirable outcome. At the same time, the results from our own and other research might also point out that these so-called anti-tumor drugs for inhibition of migration and invasion should be carefully distinguished in relation to whether they are involved in EMT and MET processes or not. If the conditions allow, examination of circulating tumor cells will be more significant to assess the effect of drugs before treatment. Most importantly, we identify that GSK-3 is not only a downstream effector but also an upstream regulator of the PI3K/AKT pathway.

Acknowledgements

This study was supported by the National Natural Science Foundation of China (no. 812-72936 and no. 81602215) and Shanghai Nature Science Foundation (no. 17ZR1417300).

Disclosure of conflict of interest

None.

Address correspondence to: Yu Zhu and Chenghe Wang, Department of Urology, Ruijin Hospital Affiliated to Medical School of Shanghai Jiaotong University, Number 197, Ruijin'er Road, Huangpu District, Shanghai 200001, China. E-mail: zhuyuruijin@163.com (YZ); wangch8603@163.com (CHW)

References

[1] Stenstrom G and Svardsudd K. Pheochromocytoma in Sweden 1958-1981. An analysis of the National Cancer Registry Data. Acta Med Scand 1986; 220: 225-232.

[2] Beard CM, Sheps SG, Kurland LT, Carney JA, Lie JT. Occurrence of pheochromocytoma in Rochester, Minnesota, 1950 through 1979. Mayo Clin Proc 1983; 58: 802-804.

[3] Pacak K, Eisenhofer G, Ahlman H, Bornstein SR, Gimenez-Roqueplo AP, Grossman AB, Kimura N, Mannelli M, McNicol AM, Tischler AS; International Symposium on Pheochromocytoma. Pheochromocytoma: recommendations for clinical practice from the First International Symposium. October 2005. Nat Clin Pract Endocrinol Metab 2007; 3: 92-102.

[4] Edstrom Elder E, Hjelm Skog AL, Hoog A, Hamberger B. The management of benign and malignant pheochromocytoma and abdominal paraganglioma. Eur J Surg Oncol 2003; 29: 278-283.

[5] Schurmeyer T, Dralle H, Schuppert F, von zur Mühlen A. [Preoperative diagnosis of suspected pheochromocytoma--retrospective assessment of diagnostic criteria]. Acta Med Austriaca 1988; 15: 106-108.

[6] Walther MM, Keiser HR and Linehan WM. Pheochromocytoma: evaluation, diagnosis, and treatment. World J Urol 1999; 17: 35-39.

[7] Kopf D, Goretzki PE and Lehnert H. Clinical management of malignant adrenal tumors. J Cancer Res Clin Oncol 2001; 127: 143-155.

[8] Wangberg B, Muth A, Khorram-Manesh A, Jansson S, Nilsson O, Forssell-Aronsson E, Tisell L, Ahlman H. Malignant pheochromocytoma in a population-based study: survival and clinical results. Ann N Y Acad Sci 2006; 1073: 512-516.

[9] Mehlen P and Puisieux A. Metastasis: a question of life or death. Nat Rev Cancer 2006; 6: 449-458.

[10] Iqbal W, Alkarim S, AlHejin A, Mukhtar H, Saini KS. Targeting signal transduction pathways of cancer stem cells for therapeutic opportunities of metastasis. Oncotarget 2016; 7: 76337-76353.

[11] Kuriyama S and Mayor R. Molecular analysis of neural crest migration. Philos Trans R Soc Lond B Biol Sci 2008; 363: 1349-1362.

[12] Yilmaz M and Christofori G. EMT, the cytoskeleton, and cancer cell invasion. Cancer Metastasis Rev 2009; 28: 15-33.

[13] Gialeli C, Theocharis AD and Karamanos NK. Roles of matrix metalloproteinases in cancer progression and their pharmacological targeting. FEBS J 2011; 278: 16-27.

[14] Waldmann J, Slater EP, Langer P, Buchholz M, Ramaswamy A, Walz MK, Schmid KW, Feldmann G, Bartsch DK, Fendrich V. Expression of the transcription factor snail and its target gene twist are associated with malignancy in pheochromocytomas. Ann Surg Oncol 2009; 16: 1997-2005.

[15] Ohta S, Lai EW, Pang AL, Brouwers FM, Chan WY, Eisenhofer G, de Krijger R, Ksinantova L, Breza J, Blazicek P, Kvetnansky R, Wesley RA, Pacak K. Downregulation of metastasis suppressor genes in malignant pheochromocytoma. Int J Cancer 2005; 114: 139-143.

[16] Lin D, Li X, Xu L, Lian J, Xu Y, Meng L, Xie X, Wang X, He H, Xu D, Wang C, Zhu Y. Apogossypolone (ApoG2) induces ROS-dependent apoptosis and reduces invasiveness of PC12 cells in vitro and in vivo. Am J Transl Res 2017; 9: 3990-4002.

[17] Li LC, Okino ST, Zhao H, Pookot D, Place RF, Urakami S, Enokida H, Dahiya R. Small dsRNAs induce transcriptional activation in human cells. Proc Natl Acad Sci U S A 2006; 103: 17337-17342.

[18] Lamouille S, Connolly E, Smyth JW, Akhurst RJ, Derynck R. TGF-beta-induced activation of mTOR complex 2 drives epithelial-mesenchymal transition and cell invasion. J Cell Sci 2012; 125: 1259-1273.
[19] Derynck R and Zhang YE. Smad-dependent and Smad-independent pathways in TGF-beta family signalling. Nature 2003; 425: 577-584.
[20] Shahjee HM, Koch KR, Guo L, Zhang CO, Keay SK. Antiproliferative factor decreases Akt phosphorylation and alters gene expression via CKAP4 in T24 bladder carcinoma cells. J Exp Clin Cancer Res 2010; 29: 160.
[21] Liu S, Li Y, Lin T, Fan X, Liang Y, Heemann U. High dose human insulin and insulin glargine promote T24 bladder cancer cell proliferation via PI3K-independent activation of Akt. Diabetes Res Clin Pract 2011; 91: 177-182.
[22] Nieman MT, Prudoff RS, Johnson KR, Wheelock MJ. N-cadherin promotes motility in human breast cancer cells regardless of their E-cadherin expression. J Cell Biol 1999; 147: 631-644.
[23] Anastas JN and Moon RT. WNT signalling pathways as therapeutic targets in cancer. Nat Rev Cancer 2013; 13: 11-26.
[24] Hennig G, Lowrick O, Birchmeier W, Behrens J. Mechanisms identified in the transcriptional control of epithelial gene expression. J Biol Chem 1996; 271: 595-602.
[25] Lamouille S, Xu J and Derynck R. Molecular mechanisms of epithelial-mesenchymal transition. Nat Rev Mol Cell Biol 2014; 15: 178-196.
[26] Bakin AV, Tomlinson AK, Bhowmick NA, Moses HL, Arteaga CL. Phosphatidylinositol 3-kinase function is required for transforming growth factor beta-mediated epithelial to mesenchymal transition and cell migration. J Biol Chem 2000; 275: 36803-36810.
[27] Bonora M, Wieckowsk MR, Chinopoulos C, Kepp O, Kroemer G, Galluzzi L, Pinton P. Molecular mechanisms of cell death: central implication of ATP synthase in mitochondrial permeability transition. Oncogene 2015; 34: 1608.
[28] Darrington RS, Campa VM, Walker MM, Bengoa-Vergniory N, Gorrono-Etxebarria I, Uysal-Onganer P, Kawano Y, Waxman J, Kypta RM. Distinct expression and activity of GSK-3alpha and GSK-3beta in prostate cancer. Int J Cancer 2012; 131: E872-883.
[29] Talmadge JE and Fidler IJ. AACR centennial series: the biology of cancer metastasis: historical perspective. Cancer Res 2010; 70: 5649-5669.
[30] Hanahan D and Weinberg RA. Hallmarks of cancer: the next generation. Cell 2011; 144: 646-674.
[31] Yang J, Mani SA, Donaher JL, Ramaswamy S, Itzykson RA, Come C, Savagner P, Gitelman I, Richardson A, Weinberg RA. Twist, a master regulator of morphogenesis, plays an essential role in tumor metastasis. Cell 2004; 117: 927-939.
[32] Ansieau S, Bastid J, Doreau A, Morel AP, Bouchet BP, Thomas C, Fauvet F, Puisieux I, Doglioni C, Piccinin S, Maestro R, Voeltzel T, Selmi A, Valsesia-Wittmann S, Caron de Fromentel C, Puisieux A. Induction of EMT by twist proteins as a collateral effect of tumor-promoting inactivation of premature senescence. Cancer Cell 2008; 14: 79-89.
[33] Ozawa M and Kobayashi W. Reversibility of the Snail-induced epithelial-mesenchymal transition revealed by the Cre-loxP system. Biochem Biophys Res Commun 2015; 458: 608-613.
[34] Chui MH. Insights into cancer metastasis from a clinicopathologic perspective: epithelial-mesenchymal transition is not a necessary step. Int J Cancer 2013; 132: 1487-1495.
[35] Scheel C and Weinberg RA. Cancer stem cells and epithelial-mesenchymal transition: concepts and molecular links. Semin Cancer Biol 2012; 22: 396-403.
[36] Miles FL, Pruitt FL, van Golen KL, Cooper CR. Stepping out of the flow: capillary extravasation in cancer metastasis. Clin Exp Metastasis 2008; 25: 305-324.
[37] Orlichenko LS and Radisky DC. Matrix metalloproteinases stimulate epithelial-mesenchymal transition during tumor development. Clin Exp Metastasis 2008; 25: 593-600.
[38] Banyard J, Chung I, Migliozzi M, Phan DT, Wilson AM, Zetter BR, Bielenberg DR. Identification of genes regulating migration and invasion using a new model of metastatic prostate cancer. BMC Cancer 2014; 14: 387.
[39] Chaffer CL, Brennan JP, Slavin JL, Blick T, Thompson EW, Williams ED. Mesenchymal-to-epithelial transition facilitates bladder cancer metastasis: role of fibroblast growth factor receptor-2. Cancer Res 2006; 66: 11271-11278.
[40] Banyard J, Chung I, Wilson AM, Vetter G, Le Béchec A, Bielenberg DR, Zetter BR. Regulation of epithelial plasticity by miR-424 and miR-200 in a new prostate cancer metastasis model. Sci Rep 2013; 3: 3151.
[41] Ocana OH, Corcoles R, Fabra A, Moreno-Bueno G, Acloque H, Vega S, Barrallo-Gimeno A, Cano A, Nieto MA. Metastatic colonization requires the repression of the epithelial-mesenchymal transition inducer Prrx1. Cancer Cell 2012; 22: 709-724.

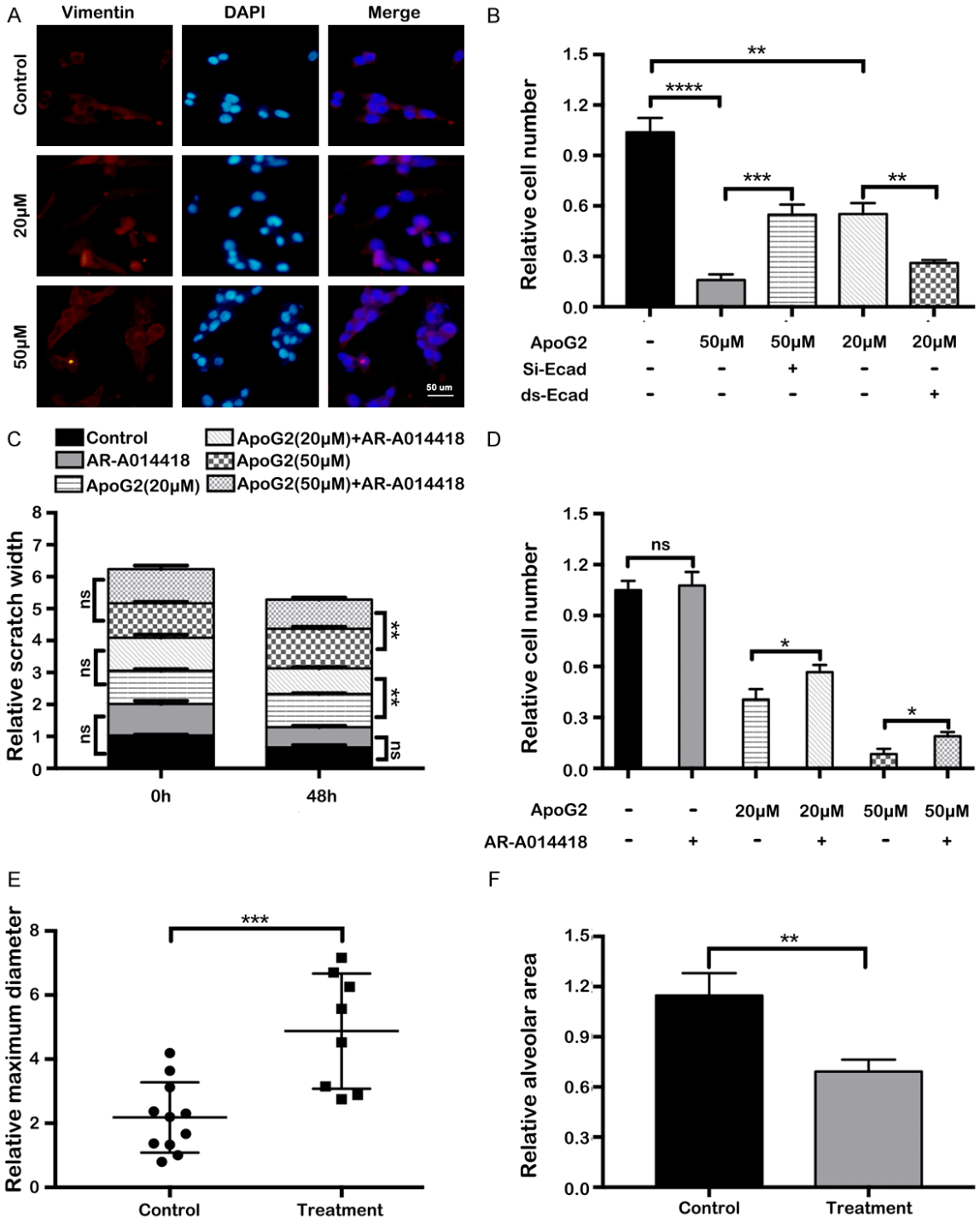

Supplementary Figure 1. A. Distribution of vimentin assessed by immunofluorescence staining. B. Statistical analysis of transwell assay results under different levels of E-cadherin. C, D. Statistical analysis of wound healing and transwell assay results with and without AR-A014418. E. Maximum diameters of metastatic foci quantified via Image J software. F. Alveolar areas in a fixed-size of field quantified via Image J software. ns, $P > 0.05$; *, $P < 0.05$; **, $P < 0.01$; ***, $P < 0.001$; ****, $P < 0.0001$.